Fluoride Ion Receptors Based on Dipyrrolyl Derivatives Bearing Electron-Withdrawing Groups: Synthesis, Optical and Electrochemical Sensing, and Computational Studies

Tamal Ghosh and Bhaskar G. Maiya[†]

School of Chemistry, University of Hyderabad, Hyderabad 500 046, India

Ming Wah Wong*

Department of Chemistry, National University of Singapore, 3 Science Drive 3, Singapore 117543

Received: August 9, 2004; In Final Form: October 1, 2004

Two dipyrrolyl derivatives, 2,3-di(1*H*-2-pyrrolyl)-7,12-dihydronaphtho[2,3-f]quinoxaline-7,12-dione (**1**) and 5,6-di(1*H*-2-pyrrolyl)-2,3-pyrazine-dicarbonitrile (**2**), bearing electron-withdrawing quinone or dicyano subunits, have been synthesized and fully characterized by various spectroscopic and electrochemical methods. Both **1** and **2** are specific binders of F^- in organic solvents and show dramatic, binding-induced changes in their color (observable in the naked-eye experiments) and also optical and electrochemical signatures. These F^--induced color changes remain the same even in the presence of a large excess of Cl^-, Br^-, I^-, or ClO_4^-, thus rendering **1** and **2** to be efficient fluoride ion sensors. While K_a for F^- binding by receptor **1** is $\sim 1.6 \times 10^4$ M^{-1}, that for receptor **2** is an order of magnitude higher. ^1H NMR titrations were carried out to monitor the binding of **1**/**2** with F^-. These experiments not only provide evidence for the hydrogen-bonding interaction between the pyrrolic NH groups of these receptors and F^-, but also offer some key insights into the structures of the receptor−anion complexes. Further insights into the structures of the receptor−anion complexes and the observed binding discrimination have been obtained by density functional calculations. Both receptors **1** and **2** interact with a halide ion by forming two NH···X^- hydrogen bonds with the pyrrolic NH protons in a bidentate fashion. The predicted order of halide binding affinity for receptors is $F \gg Cl > Br$. The high selectivity for F^- among the halides is attributed mainly to the strength of the hydrogen bond and partly to the complementarity of the geometries between the receptor and anion. The higher F^- binding ability of **2** over **1** has been interpreted in terms of the greater electron deficiency and enhanced hydrogen-bond-donating character of the former derivative. Calculations of the NMR and UV−visible spectra support the experimental characterization of the receptor−anion complexes.

1. Introduction

Inorganic anions play an important role in various industrial processes, energy transduction and enzymatic activity in organisms, clinical treatment of various disease states, etc.[1−5] Sensing such anions is a challenging area in chemistry. Indeed, it is only recently that the coordination chemistry of anions is being developed as opposed to that of cations. Among the many inorganic anions, fluoride ion is drawing a special attention due to its beneficial (e.g., prevention of dental caries and treatment of osteoporosis)[6,7] as well as detrimental (e.g., fluorosis)[8] roles. Thus, a wide variety of optical and electrochemical F^- sensors based on either positively charged or neutral organic receptors have been reported to date.[1−5] Of specific relevance to the present work are the recently reported pyrrole-based sensors, calix[4]pyrrole[9,10] and dipyrrolylquinoxaline (DPQ)[11−18] families of compounds. The latter sensors have the dual advantage of possessing a built-in chromophore and being readily accessible in two steps from commercially available materials. In addition, introduction of electron-withdrawing groups at the pyrrole or quinoxaline subunits of the DPQ moiety is known to result in enhanced binding of the anion with the receptor.[11−14] Combing these attractive structural and spectroscopic features of dipyrrolyl derivatives will, therefore, provide ample opportunities to synthesize variously substituted DPQ and related classes of motifs and develop anion sensors that suit individual application. Our efforts in this research area resulted in the synthesis of two new dipyrrolyl receptors **1** and **2**, both of which were found to be avid binders of F^-.[18] As will be described in this paper, the highlights of this work are (i) both **1** and **2** sense F^- by naked eye and optical and electrochemical detection methods, (ii) these receptors (especially **1**) show dramatic, fluoride ion binding-induced changes in their optical signatures even in the presence of excess Cl^-, Br^-, I^-, and ClO_4^-, and (iii) **1** and **2** are the first set of the dipyrrolylpyrazine (DPP)/DPQ class of compounds, of which the receptor activities are investigated by quantum mechanical methods.[19] This computational study provides not only insight into the structures, intrinsic binding affinities, and the underlying intermolecular interactions of the receptor−anion complexes, but also supports the experimental characterization via computations of NMR and UV−visible spectra.

2. Experimental Section

2.1. Materials. All anions, in the form of tetrabutylammonium salts, were purchased from Sigma-Aldrich Chemical Co., stored in a desiccator under vacuum containing self-indicating silica, and used without any further purification. Pyrrole

* Corresponding author. Fax: (+61) 67791691. E-mail: chmwmw@nus.edu.sg.

† Deceased.

10.1021/jp0464223 CCC: $27.50
Published on Web 11/23/2004

(Ranbaxy Across, Belgium) was dried over CaH_2 (Ranbaxy, Mumbai, India) and distilled under nitrogen. All solvents, including the HPLC-grade solvents, used in the spectroscopic and electrochemical studies were purchased from Ranbaxy (Mumbai, India) and were distilled as per requirement by the published procedures.[20] $CDCl_3$, CD_3OD, and $(CD_3)_2SO$ were purchased from Merck (Germany).

1,2-Di(1*H*-2-pyrrolyl)-1,2-ethanedione (**3**) was prepared by a procedure published elsewhere.[11,21] The two new receptors investigated in this study were synthesized as detailed below.

*2,3-Di(1H-2-pyrrolyl)-7,12-dihydronaphtho[2,3-f]quinoxaline-7,12-dione (**1**).* The diketone **3** (100 mg, 0.53 mmol) was dissolved in glacial acetic acid (40 mL), and a solution of 1,2-diaminoanthraquinone (190 mg, 0.8 mmol) in acetic acid (30 mL) was added with stirring. The resulting mixture was heated at reflux under nitrogen atmosphere for 12 h. The major part of acetic acid was then distilled off under vacuum, and the residue was taken up in a mixture of $CHCl_3$ (50 mL) and water (50 mL). The organic layer was separated off, and the aqueous layer was extracted with $CHCl_3$ (3 × 30 mL). The organic layers were combined and washed successively with saturated aqueous sodium bicarbonate solution (50 mL), water (50 mL), and brine (50 mL). The solution was then dried over anhydrous sodium sulfate, filtered, and evaporated to dryness. Silica gel column chromatography (eluent: $CHCl_3$/EtOAc, 96:4, v/v) afforded **1** (170 mg, 82%) as a red solid. Anal. Calcd for $C_{24}H_{14}N_4O_2$: C, 73.84; H, 3.61; N, 14.35. Found: C, 73.78; H, 3.65; N, 14.25. ^{1}H NMR (200 MHz, $(CD_3)_2SO$, TMS) δ, ppm: 6.19−6.25 (2H, m, pyrrole H), 6.50−6.53 (1H, m, pyrrole H), 6.64−6.66 (1H, m, pyrrole H), 7.12−7.17 (2H, m, pyrrole H), 7.88−8.00 (2H, m, naphthyl H), 8.19−8.22 (2H, m, naphthyl H), 8.25 (1H, d, $^3J_{H-H}$ = 10 Hz, quinoxaline H), 8.40 (1H, d, $^3J_{H-H}$ = 10 Hz, quinoxaline H), 11.16 (1H, br s, NH), 11.87 (1H, br s, NH). ^{13}C NMR (50 MHz, $(CD_3)_2SO$, TMS) δ, ppm: 114.7, 114.9, 118.4, 119.1, 128.3, 128.8, 130.5, 131.4, 131.7, 132.9, 133.3, 133.9, 137.1, 138.7, 138.9, 139.8, 140.1, 147.3 (some lines are overlapping, giving rise to less number of signals). mp: >250 °C. FAB-MS (M/Z^+): 392 $(M + 2H)^+$. UV−visible (CH_2Cl_2) λ_{max}, nm (ϵ, M^{-1} cm^{-1}): 290 (26 640), 508 (12 410). IR (KBr pellet, cm^{-1}): 3376, 1665.

*5,6-Di(1H-2-pyrrolyl)-2,3-pyrazinedicarbonitrile (**2**).* The diketone **3** (150 mg, 0.8 mmol) and 1,2-diaminomaleonitrile (121 mg, 1.12 mmol) were dissolved in ethanol (50 mL), and a catalytic amount of BF_3·Et_2O was added to this solution. It was then heated at reflux under nitrogen atmosphere for 8 h. The solvent was then removed, and the residue was dissolved in CH_2Cl_2 and filtered. The filtrate was chromatographed over silica gel column (eluent: CH_2Cl_2/EtOAc, 99:1, v/v)) to afford **2** (162 mg, 78%) as a yellow solid. Anal. Calcd for $C_{14}H_8N_6$: C, 64.61; H, 3.10; N, 32.30. Found: C, 64.55; H, 3.02; N, 32.21. ^{1}H NMR (200 MHz, $CDCl_3$, TMS) δ, ppm: 6.30−6.34 (2H, m, pyrrole H), 7.11−7.14 (2H, m, pyrrole H), 7.35−7.39 (2H, m, pyrrole H), 9.61 (2H, br s, NH). ^{13}C NMR (50 MHz, $CDCl_3$/CD_3OD, 4:1, v/v, TMS) δ, ppm: 112.0, 115.4, 116.9, 126.6, 126.9, 127.9, 145.4. mp: 185 ± 1 °C (reported: 186 °C). FAB-MS (M/Z^+): 260. UV−visible (CH_2Cl_2) λ_{max}, nm (ϵ, M^{-1} cm^{-1}): 338 (18 690), 427 (18 890). IR (KBr pellet, cm^{-1}): 3314, 2243.

2.2. Methods. Care was taken to avoid the entry of direct, ambient light into the samples in all of the spectroscopic and electrochemical experiments described below. Unless otherwise specified, all of the experiments were carried out at 298 ± 1 K.

The ^{1}H and ^{13}C NMR spectra were recorded on a Bruker NR-200 AF-FT NMR spectrometer using tetramethylsilane (TMS) as an internal standard. UV−visible spectra were recorded on a Shimadzu UV-3101 PC spectrophotometer. A matched pair of quartz cuvettes (path length = 1 cm) was employed for this purpose. Steady-state fluorescence spectra were recorded in a four-walled, all-transparent, quartz cell (path length = 1 cm) using a Spex model FluoroMax-3 (Jobin Yvon-Spex) spectrofluorimeter for solutions having optical densities at the wavelengths of excitation (λ_{ex}) ~0.2, with excitation and emission slits of 3 nm each. The emitted quanta were detected at right angle to the incident beam. The fluorescence quantum yields (ϕ) were estimated by integrating the fluorescence bands and by using either 5,10,15,20-tetraphenylporphyrin (H_2TPP) (ϕ = 0.13 in CH_2Cl_2)[22] or 1,6-diphenyl-1,3,5-hexatriene (ϕ = 0.80 in cyclohexane)[23] as the standards. Cyclic- (CV) and differential pulse (DPV) voltammetric experiments were carried out on a CH instruments model CHI 620A electrochemical analyzer, as detailed in our previous studies (working and auxiliary electrodes, Pt; reference electrode, Ag).[24−28] Fc^+/Fc (Fc = ferrocene) couple was used to calibrate the redox potential values, which are reported in V vs SCE $E_{1/2}$ for the Fc^+/Fc couple. The Fc^+/Fc couple was found to be 0.48 V vs SCE in DMF, 0.1 M $TBAPF_6$ under our experimental conditions.

Absorption and Fluorescence Titration Studies. Absorption titrations of sensors **1** and **2** against different anions were carried out in the following way: CH_2Cl_2 solution containing **1** or **2** (typically 10 μM) was taken in the cuvette and titrated with an increasing volume of concentrated solution of a given anion. The change in absorbance at 650 nm for **1** and 480 nm for **2** was plotted against anion concentration and fitted by the equation as described by Connors,[29]

$$\Delta A/b = (Q_t K_a \Delta\epsilon[L])/(1 + K_a[L]) \quad (1)$$

where ΔA refers to the change in absorbance from the initial value at the required wavelength, b is the cuvette path length (in cm), Q_t is the total concentration of sensors, K_a is the binding constant, $\Delta\epsilon$ is the change in extinction coefficient between free and bound sensor, and [L] is the concentration of titrated anion.

Fluorescence titrations were carried out by exciting the sensors **1** and **2** at 510 and 430 nm, respectively, and monitoring the intensity at the emission maximum of the respective sensors (typically 10 μM). The dependence of I/I_0 upon anion concentration is described by the equation,[29]

$$I/I_0 = (1 + (k_f/k_s)K_a[L])/(1 + K_a[L]) \quad (2)$$

where I_0 refers to the fluorescence intensity due to the sensor in the absence of any anion, I is its intensity upon addition of the given anion, k_f is the proportionality constant of the bound sensor, k_s is the proportionality constant of the free sensor, K_a is the binding constant, and [L] is the concentration of titrated anion.

^{1}H NMR Titrations. Sensor **1** (2.56×10^{-2} M in $(CD_3)_2SO$) was titrated against F^- (tetrabutylammonium fluoride, TBAF) by incremental additions of a concentrated solution of the anion in $(CD_3)_2SO$ such that, at the end of the titration, [**1**]:[F^-] = 1:5. Sensor **2** (3.84×10^{-2} M in $CDCl_3$) was also titrated against F^- in a similar manner ([**2**]:[F^-] = 1:1.5).

Electrochemical Titrations. CV and DPV traces were recorded for solutions (DMF, 0.1 M $TBAPF_6$) of sensors **1** or **2**, with and without added anion. In a typical titration experiment, a solution containing 5.0×10^{-4} M of **1** or 2.0×10^{-3} M of **2** was titrated against TBAF, and the redox wave was monitored by DPV.

SCHEME 1: Synthesis of Receptors 1 and 2

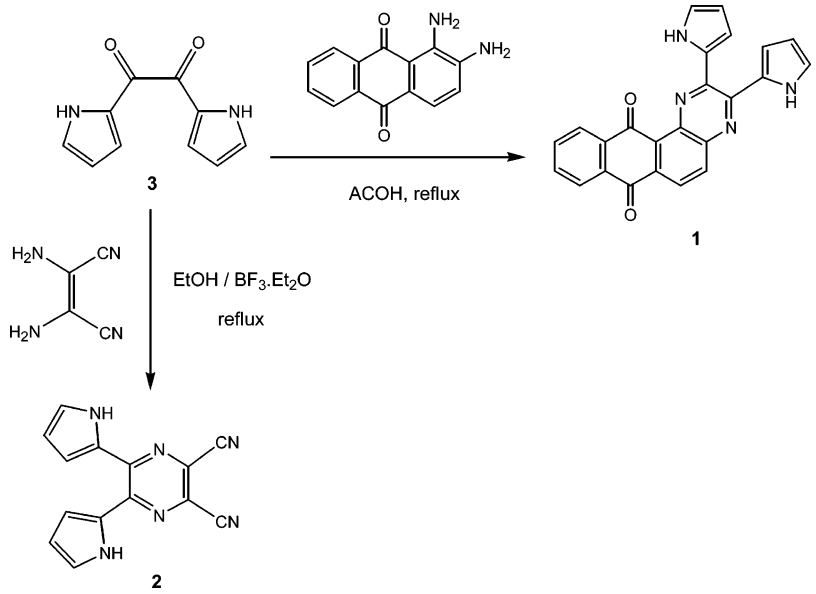

Computational Methods. The molecular complexes of **1**, **2**, pyrrole (**4**), and 2,3-di(1*H*-2-pyrrolyl)-pyrazine (**5**) with halide ions ($X^- = F$, Cl, and Br) were examined by density functional calculations. Geometry optimizations were performed at the B3LYP[30,31] level using the split-valence polarized 6-31G* basis set. Higher-level relative energies were computed at the B3LYP/6-311+G** level based on the B3LYP/6-31G* optimized geometries and include the zero-point energy (ZPE) correction (B3LYP/6-31G* value, scaled by a factor of 0.9804).[32] The interaction (or binding) energy (ΔE_{int}) of the receptor−anion complex was computed using eq 3 as the difference between the energy of the complex ($E_{[R\cdots X^-]}$) and the total energy of the two free monomers, that is, receptor (E_R) and halide ion (E_{X^-}).

$$\Delta E_{int} = E_{[R\cdots X^-]} - (E_R + E_{X^-}) \quad (3)$$

The free energy differences (ΔG) were computed from the equation $\Delta G_T = \Delta H_T - T\Delta S$, where ΔS is the entropy change and $\Delta H_T = \Delta H_0 + (H_T - H_0)$. The thermal correction ($H_{298} - H_0$) and entropy values (S_{298}) of the halide anions were taken from the JANAF compilation.[33] We have examined the effect of basis set superposition error (BSSE) on the binding energies of the **2**···F^- and **2**···Cl^- complexes using the counterpoise method[34] and found that the magnitude of BSSE is relatively small, less than 2 kJ mol^{-1}. Hence, our calculated interaction energies do not include BSSE correction.

For all investigated species, a charge density analysis was performed using the natural bond orbital (NBO) approach based on the B3LYP/6-31G* wave function.[35] NBO atomic charges of small molecules have recently been demonstrated to agree well with experimental values obtained from X-ray diffraction data.[36] NMR shielding tensors spectra of **1**, **2**, and their fluoride ion complexes were computed with the gauge-independent atomic orbital (GIAO) method.[37,38] The proton chemical shifts, with reference to TMS, were computed at the B3LYP/6-311+G-(2d,p) level. The transition energies of receptors **2** and **5** and their halide−ion complexes were calculated using the time-dependent DFT (TD-DFT) method[39,40] at the B3LYP/cc-pVTZ level. All calculations were performed using the Gaussian 98 series of programs.[41]

3. Results and Discussion

Structurally, while receptor **1** can be considered as a DPQ derivative having the quinone moiety as part of its extended π framework, compound **2** is a newly introduced receptor motif, dipyrrolylpyrazine (DPP),[42] that is substituted with two cyano groups directly on its skeleton. The rationales behind the introduction of a quinone or cyano group in these sensors are 2-fold: (i) these strongly electron-withdrawing groups are expected to render the pyrrolic nitrogens highly acidic and thereby enhance the hydrogen-bonding ability of the anionic receptors,[11−14] and (ii) both quinone and cyano substituents are redox active,[27,28] and, hence, the anion binding event can be monitored by the electrochemical methods as well.

The schemes leading to the synthesis of sensors **1** and **2** are illustrated in Scheme 1. Reaction of easily synthesizable 1,2-di(1*H*-2-pyrrolyl)-1,2-ethanedione (**3**)[11,21] with commercially available 1,2-diaminoanthraquinone or 1,2-diaminomaleonitrile readily furnished receptors **1** and **2**, respectively, in ∼80% yield in each case. These two compounds are sufficiently characterized for their purity and structural integrity by elemental analysis, FAB-MS, IR, UV−visible, and ^1H (1D and $^1H-^1H$ COSY) and ^{13}C NMR methods, as described in the Experimental Section.

3.1. Spectral and Electrochemical Characterization of Receptors. The mass, infrared, UV−visible, and NMR data of the new sensors are summarized in the Experimental Section. The infrared spectrum of receptor **1** shows peaks at 3376 and 1665 cm^{-1} ascribable to the pyrrolic NH and quinone carbonyl stretching frequencies, respectively. Similarly, the peaks appearing at 3314 and 2243 cm^{-1} in the spectrum of **2** indicate the presence of pyrrolic NH and cyano groups, respectively. Based on the data of several previously reported dppz (=dipyrido[3,2-a:2′,3′-c]phenazine)-based ligands[27,28,43,44] and DPQ-based sensors,[11−17] as well as our UV calculations, peaks observed in the UV−visible spectra of **1** and **2** are assigned to various $\pi \rightarrow \pi^*$ transitions. Both of the new receptors are found to show fluorescence (CH_2Cl_2, λ_{em}, nm: **1**, 693 and **2**, 541). These fluorescence bands were found to be broad (full-widths at half-maximum, fwhm (cm^{-1}): **1**, 3075 and **2**, 3903), and it was not possible to assign these bands unambiguously. Interestingly, however, the fluorescence quantum yield (ϕ) of **2** is found to be higher (0.41) than that of **1** (0.015) in CH_2Cl_2.

Figure 1 illustrates the ^1H NMR spectra of receptors **1** and **2**. The spectra were analyzed (see Experimental Section) on the basis not only of the chemical shift and integrated intensity data of the various peaks appearing in the 1D spectra but also of the proton connectivity patterns observed in the corresponding

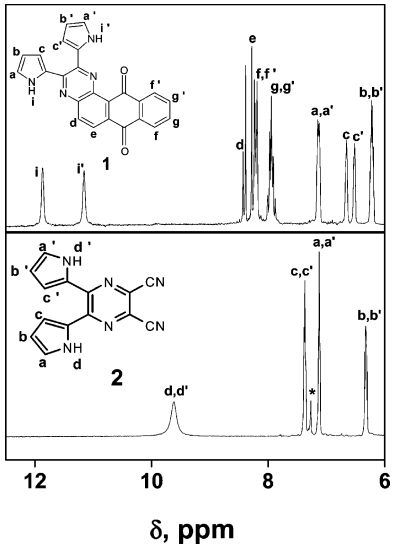

Figure 1. ^{1}H NMR spectra of receptors **1** ($(CD_3)_2SO$, TMS) and **2** ($CDCl_3$, TMS). ∗ indicates the solvent signal for $CDCl_3$.

^{1}H−^{1}H COSY spectra. The assignments made on the basis of these analyses are consistent with the proposed structures of the new receptors. Interestingly, while the two β-pyrrole protons of **1** (2.56×10^{-2} M in $(CD_3)_2SO$) resonate as two distinct signals at 6.52 and 6.65 ppm, the corresponding protons of **2** (3.84×10^{-2} M in $CDCl_3$) appear at 7.37 ppm. Our calculated ^{1}H NMR spectrum of **1** shows that the two pyrrole rings are significantly different, particularly for the β protons (see Theoretical Calculations).

In the cyclic voltammetric experiments (DMF, 0.1 M $TBAPF_6$), while receptor **1** showed one reversible ($E_{pa} - E_{pc} = \Delta E_p = 70$ mV and $i_{pc}/i_{pa} = 0.98$) and one quasi-reversible ($\Delta E_p = 138$ mV and $i_{pc}/i_{pa} = 0.7$ in the scan rate (ν) over the range of 100−500 mV s^{-1}) current−voltage response at −0.51 and −0.76 V (vs SCE), compound **2** showed a quasi-reversible peak ($\Delta E_p = 94$ mV) with the cathodic peak appearing at −1.13 V at a scan rate of 100 mV s^{-1}.[45]

3.2. Anion Sensing. We envisaged that given the novel built-in structural features, notably, the presence of highly withdrawing groups in **1** and **2**, it should be possible to monitor the fluoride ion binding properties of these receptors by colorimetric, fluorimetric, and electrochemical methods, thus enhancing the utility of this class of compounds in anion sensing applications. Indeed, as will be discussed below, both **1** and **2** are avid binders of F^- in organic solvents and show dramatic, binding-induced changes in their optical signatures even in the presence of excess Cl^-, Br^-, I^-, or ClO_4^-.

3.2.1. Colorimetric Experiments. In the naked-eye colorimetric experiments, receptors **1** and **2** (1×10^{-4} M in CH_2Cl_2 or DMSO) show dramatic color changes from red to green and from yellow to orange-red, respectively, in the presence of TBAF (3×10^{-3} M); see Figure 2. While receptor **1** was found to be insensitive to the addition of any other anion (up to ∼1000 mol equiv excess) employed during this study, receptor **2** produced a faint orange-red color in the presence of $H_2PO_4^-$ (9×10^{-3} M) but did not change its color upon addition of excess Cl^-, Br^-, I^-, and ClO_4^-. Moreover, addition of F^- (3×10^{-3} M) to those solutions of **1** (1×10^{-4} M) containing excess Cl^-, Br^-, I^-, ClO_4^-, or $H_2PO_4^-$ immediately generated the expected green color, suggesting that **1** is a very specific binder of F^-. The situation is quite similar to **2** where this receptor senses F^- in the presence of excess Cl^-, Br^-, I^-, and ClO_4^-.

3.2.2. UV−Visible Experiments. Figure 3 displays the changes in the UV−visible spectra of **1** and **2** observed upon the addition of F^- in CH_2Cl_2 solutions. Peaks at 290 and 508 nm of **1** decrease upon addition of TBAF, and new peaks appear at 260, 327, and 650 nm (Figure 3A). On the other hand, peaks at 338 and 427 nm are shifted to 358 and 469 nm, respectively, for **2** in the presence of F^- (Figure 3B). The inset figure in each panel is the best fit to eq 1 for the plot of change in absorbance against [F^-]. It indicates the mode of binding between sensors and F^- as 1:1 (see Figure S1, Supporting Information). Similar sets of titrations were carried out for **1** and **2** with the other anions investigated in this study, and the apparent binding constants (K_a) extracted using eq 1 are summarized in Table 1.

Data given in Table 1 reveal the following: (i) among all of the anions, F^- binds strongly with both of the sensors, (ii) while K_a for F^- binding by receptor **1** is as high as $\sim 1.6 \times 10^4$ M^{-1}, and that for receptor **2** is an order of magnitude higher, and (iii) while $H_2PO_4^-$ shows relatively low binding constants with **2**, receptor **1**, on the other hand, does not bind to any other anion except F^-. An important additional observation made during these experiments is that the spectra (and also the color of the solution) of receptor−F^- conjugates revert back to the original spectra corresponding to those receptors in the absence of the anion upon addition of small aliquots of water/methanol.

Thus, the fluoride ion having the highest electronegativity and the smallest size among all of the anions being investigated here binds strongly with both **1** and **2**, as is the case with most of the DPQ derivatives reported earlier.[11−17] The higher F^- binding ability of **2** over **1** is attributed to a consequence of the greater electron deficiency and enhanced hydrogen-bond-donating character of the former derivative (see Theoretical Calculations). This enhanced hydrogen-bond-donating character of **2** is responsible for the ability of this receptor to bind, albeit weakly, to $H_2PO_4^-$. In as much as this is true, we rationalize that it is the moderate binding ability of **1** that leads to selective binding of F^- by this receptor in contrast with **2**. Generation of the original spectra of the pure receptors from those of receptor−F^- adducts upon the addition of water/methanol not only suggests that the complexation between F^- and **1**/**2** is reversible in nature but also lends further support to the proposition that hydrogen bonding is involved in the binding between the receptor and the anion.

3.2.3. Fluorescence Titration Experiments. Results of fluorescence titration experiments carried out with these receptors corroborate well with those obtained during the UV−visible titrations described above. Successive additions of F^- to CH_2Cl_2 solutions of **1** and **2** result in a decrease of their fluorescence intensities with marginal changes in the emission maxima. This is illustrated in Figure 4, which shows the fluorescence spectra of receptors **1** and **2** in the absence and presence of various concentrations of F^-. Treatment of the fluorescence intensity data using eq 2, followed by standard curve fitting (see insets in Figure 4),[29] provided the K_a values (**1**, 1.35×10^4 M^{-1} and **2**, 1.4×10^5 M^{-1}) that were comparable to those obtained in the UV−visible experiments. Fluorescence spectral profiles and the intensities of both **1** and **2** were found to be unsusceptible to the addition of other anions. The near invariance of both λ_{em} and intensity values observed during these titrations indicates that anions other than F^- interact very little with both **1** and **2**.

3.2.4. ^{1}H NMR Titration Experiments. Notwithstanding this observed agreement between the results of naked-eye, UV−visible, and fluorescence titration experiments carried out with **1** and **2**, the forces operating behind the UV−visible spectral changes (and hence the color changes) and the exact mechanism

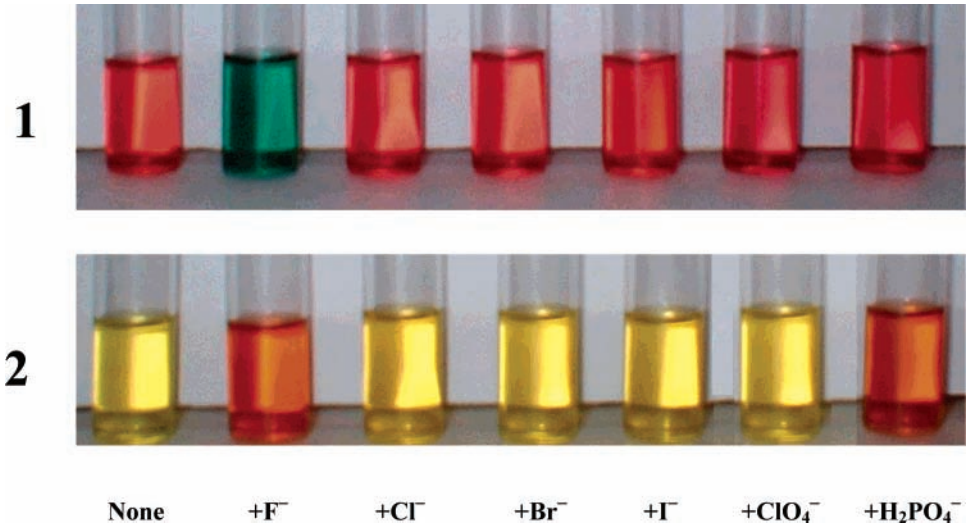

Figure 2. Color changes observed for **1** and **2** in CH_2Cl_2 upon the addition of anions as TBA salts. From left to right: none, F^-, Cl^-, Br^-, I^-, ClO_4^-, and $H_2PO_4^-$.

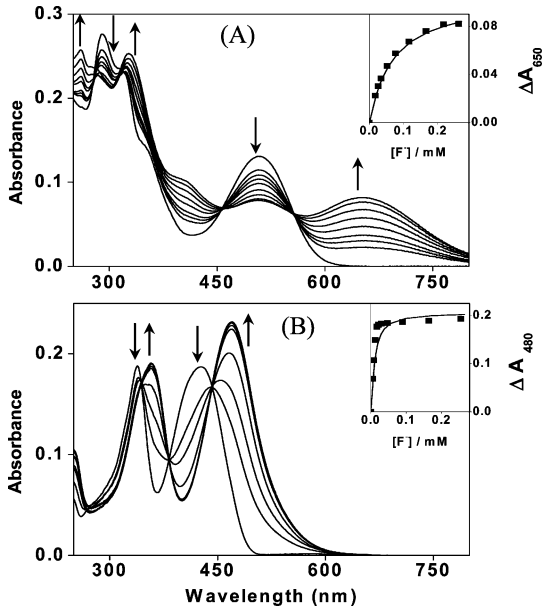

Figure 3. UV−visible spectral changes observed for (A) **1** and (B) **2**, upon addition of fluoride anion in CH_2Cl_2 at 298 K. [**1**] and [**2**] = 1.0×10^{-5} M; [TBAF] = $(0-3) \times 10^{-4}$ M. The insets show the fit of the experimental data to a 1:1 binding profile (eq 1).

TABLE 1: Anion Binding Constants (M^{-1}) for Receptors 1 and 2 in CH_2Cl_2 Determined by the Absorption Titration Method at 25 °C[a]

species	F^-	Cl^-	Br^-	I^-	ClO_4^-	$H_2PO_4^-$
1	16 000	ND[b]	ND[b]	ND[b]	ND[b]	ND[b]
2	165 000	ND[b]	ND[b]	ND[b]	ND[b]	460

[a] Countercation was tetrabutylammonium salts for all cases. All errors are ±10%. [b] Changes in the UV−visible spectra were not enough to calculate the binding constant.

of fluorescence quenching by F^- are still unclear, nor do these results provide any structural insight into the receptor−anion complexation. ^{1}H NMR spectroscopy is a versatile tool to probe such issues, and we decided to probe the interaction of receptors **1** and **2** with various anions by the ^{1}H NMR titration method, the results of which are discussed below.

At the outset, it should be noted that no major changes in the ^{1}H NMR spectra of **1** and **2** have been noticed when anions (in excess and as tetrabutylammonium salts) other than F^- were

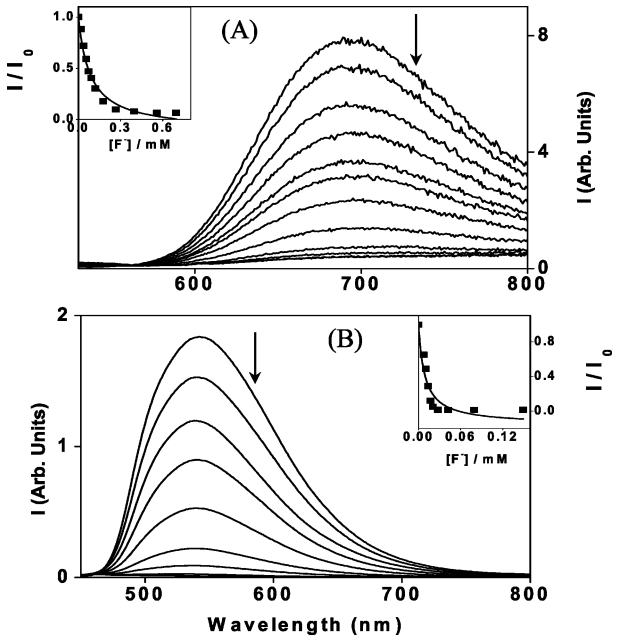

Figure 4. Fluorescence spectral changes observed for (A) **1** and (B) **2**, upon addition of fluoride anion in CH_2Cl_2 at 298 K (λ_{exc} = 510 and 430 nm, respectively). [**1**] and [**2**] = 1.0×10^{-5} M, [TBAF] = $(0-3) \times 10^{-4}$ M. The insets show the fit of the experimental data to a 1:1 binding profile.

added to $(CD_3)_2SO$ or $CDCl_3$ solutions containing these receptors. This observation is consistent with the inability of these same anions to produce changes in the absorption or emission spectra of **1** and **2**. However, dramatic effects were observed in the spectral features of these receptors in the presence of F^-. Figure 5 illustrates the ^{1}H NMR spectra of receptor **1** in the absence (A) and presence (B−E) of various concentrations of TBAF. A cursory glance of these spectra reveals that the resonances ascribable to the NH protons on **1** (11.87 and 11.16 ppm) are initially broadened upon successive addition of TBAF and finally appear at ~20.2 ppm at [**1**]:[F^-] = 1:5. A similar broadening for the NH peak in **2** (9.61 ppm) was also noticed during the initial stages of the titration, but the peak completely disappeared from the spectral window (+25 to +5.5 ppm) at [**2**]:[F^-] = 1:1.5 (see Figure S2, Supporting Information). In any case, the effect seen for the pyrrolic NH proton resonances of **1** or **2** in the presence of F^- can be regarded as evidence for

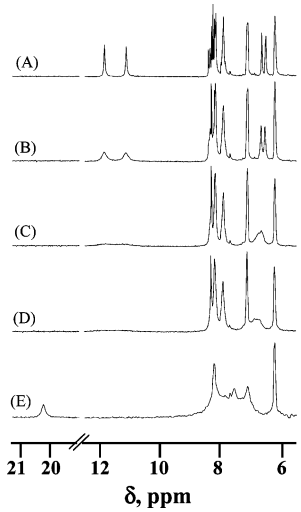

Figure 5. ^{1}H NMR titration of **1** with TBAF in $(CD_3)_2SO$; [**1**] = 2.56 × 10^{-2} M; [**1**]:[F^-] in these traces are (A) 1:0, (B) 1:0.2, (C) 1:0.6, (D) 1:1, and (E) 1:5.

the involvement of hydrogen bonding between the two acidic pyrrole NH protons of these receptors and F^-.

A careful examination of the ^{1}H NMR spectra of these receptors containing various concentrations of F^- reveals that both the α and the β protons on the pyrrole rings (and quinoxaline protons of **1**) are also shifted during the titrations. For example, the β protons of the pyrrole rings of **1** that were resonating at 6.65 and 6.52 ppm as two separate multiplets in the absence of F^- slowly broaden and resonate at ∼6.9 ppm in the presence of excess F^-. A similar broadening of the β protons of **2** was also noticed during the titration with this anion. These observations together with the interpretation made above for the NH proton resonances can be rationalized in terms of a model proposed earlier for F^- binding by various DPQ derivatives[11] and strongly supported by our calculations (see subsequent section). In this model, binding of F^- is proposed to be facilitated by rotation of the pyrrole rings of **1** and **2** in such a way that the NH protons direct toward the lone pairs of the anion. Such a rotation is expected to aid the pyrrole rings to assume a "bite angle" suitable for the size of F^- and to position them away from the quinoxaline/pyrazine chromophore leading to perturbation in the orbital overlap between the pyrrole and quinoxaline/pyrazine subunits. To the first approximation, this anion binding-induced "intramolecular" perturbation in the orbital overlap rationalizes the UV−visible, fluorescence, and NMR spectral changes observed for **1** and **2** upon binding with the fluoride ion. It also seems to explain the changes in the redox potential values observed during the F^- titrations with **1** and **2**, as discussed below.

3.2.5. Electrochemical Experiments. As mentioned earlier, one of the main motivations in introducing quinone/dicyano groups at the dipyrrolyl subunit has been to incorporate redox activity to this class of receptor molecules so that their anion sensing abilities can also be monitored by electrochemical methods. In this regard, it should be noted that electrochemical methods can, in principle, provide information about the binding properties of both the oxidized and the reduced forms of the receptors. It should also be noted that, except for a solitary exception, anion sensing by the previously reported DPQ derivatives has not been investigated by electrochemical methods. Figure 6 shows the DPV (DMF, 0.1 M $TBAPF_6$)[46] traces for receptors **1** and **2** in the absence and presence of F^-. Addition of successive amounts of F^- results in the reduction of the peak current and anodic shift of the peak potential for both of the

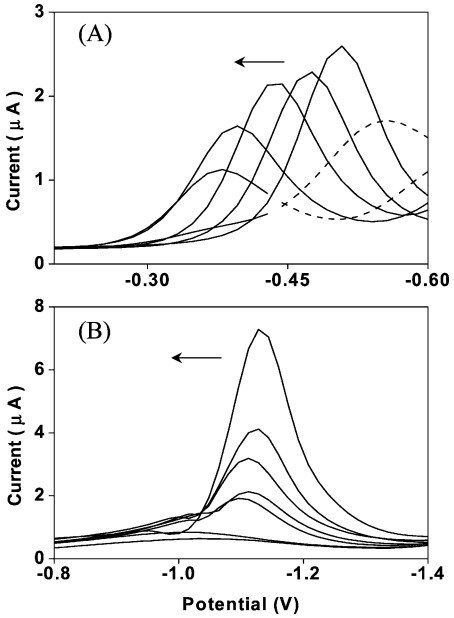

Figure 6. Differential pulse voltammograms (DMF, 0.1 M $TBAPF_6$; scan rate, 100 mV s^{-1}) of (A) **1** (5 × 10^{-4} M) and (B) **2** (2.0 × 10^{-3} M) in the presence of various concentrations of F^-. From right to left: (A) [F^-] = 0, 0.06, 0.23, 0.46, 0.84, and 2.1 mM. (B) [F^-] = 0, 0.032, 0.26, 0.74, 1.27, 2.20, and 3.68 mM. The dotted regions of the last two traces seen in panel A arise due to the second reduction peak of **1** that is anodically shifted during the titration with F^-.

SCHEME 2

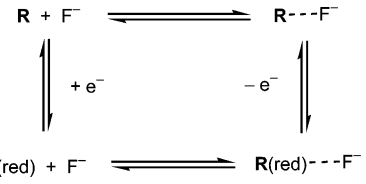

receptors. The peak, in each case, disappeared completely at the end of the titration as in the case with a cobalt(III)−dipyridophenazine complex-linked DPQ derivative reported earlier.[13] The complete disappearance of the peak for this latter complex in the presence of F^- has been interpreted in terms of a strong and, perhaps, electro-inactive complex formation between the receptor and F^-. This interpretation seems to be quite reasonable if we consider that the binding constant reported for Sessler's receptor is as high as 5.4 × 10^4 M^{-1},[13] close to the K_a values obtained for receptors **1** and **2** by the optical methods (vide infra). In any case, the successive anodic shifts of the peak potential observed for **1** and **2** in the presence of F^- permit us to evaluate the ratio of the binding constants for the neutral and one-electron-reduced receptor species as described below.[47]

The overall electrochemistry of the R−F^- (R = **1** or **2**) system can be illustrated as shown in Scheme 2. In Scheme 2, R(red) represents the one-electron-reduced species of R. Scheme 2 also suggests that the redox data can be treated according to eq 4.[48]

$$E_0^{\,f} - E_0^{\,b} = RT/nF \ln[K(\mathrm{R})/K(\mathrm{R(red)})] \qquad (4)$$

Here, $E_0^{\,f}$ and $E_0^{\,b}$ are the thermodynamic redox potentials for the free and fluoride-bound receptors, respectively, n is the number of electrons transferred, K(R)/K(R(red)) is the ratio of binding constant for the oxidized and the corresponding reduced species for R. Other parameters have their usual meaning. Substitution of appropriate values to suit the electrochemistry

of **1** and **2** in the presence of F^- and from a limiting shift of −128 mV (**1**) and −32 mV (**2**), the values of $K(R)/K(R(red))$ were calculated to be ∼0.0062 and ∼0.28, for R = **1** and **2**, respectively. These ratios, which are both less than 1, indicate that the one-electron-reduced species of **1** and **2** are better F^- receptors than the corresponding neutral species. If one considers that hydrogen bonding between the acidic NH protons of neutral **1**/**2** is involved in the binding, the <1 ratios observed for $K(R)/K(R(red))$ suggest the NH protons of the anionic species are more acidic than the neutral analogues. This apparent anomaly can perhaps be reconciled by recalling in our model that binding of fluoride leads to perturbation in the orbital overlap between the pyrrole and quinoxaline/pyrazine subunits. Perhaps, the anodic shifts of the peak potentials for the fluoride-bound sensors are a consequence of this perturbation in the orbital overlap. Note, in this regard, that the site of electron addition in these receptors is expected to be located at the quinoxaline/pyrazine parts and not the pyrrolic subunits of their structures. The pyrrolic subunits orient themselves in planes different from the plane of the quinoxaline/pyrazine part while hydrogen bonding with F^- (see sections 3.2.4, 3.3.2, and 3.3.3). Thus, the shifts observed during the redox titrations are a composite of those due to F^- binding to the NH protons and a change in the electron density distribution at the electro-active centers of these receptors. This explains the case with the apparent binding constants noted above for the one-electron-reduced receptor species.

3.3. Theoretical Calculations. To shed light on the structures, relative stabilities, and binding mechanism of the receptor−anion complexes, density functional calculations were carried out for the receptor−halide ion complexes between the receptors **1** and **2** and halides ions X^- (X = F, Cl, and Br).

*3.2.1. Structures of Anion Receptors **1** and **2**.* First, we investigate the structures and relative stabilities of the various possible conformations of the anion receptors **1** and **2**. In both cases, there are several conformations that arise from different orientations of two pyrrolyl units toward the pyrazine ring, **1a**, **1b**, **1c**, and **1d** conformations for **1**, **2a**, **2b**, and **2c** conformations for **2** (Figure 7). The calculated B3LYP/6-311+G**//B3LYP/6-31G* + ZPE relative energies are given in Figure 7. The lowest-energy conformation of **1** and **2** corresponds to the structure where both pyrrolic NH protons are facing the nitrogen atoms of pyrazine ring. This conformational preference is readily understood in terms of the favorable intramolecular NH···N hydrogen-bond interaction between the pyrrolic NH proton and the nitrogen atom of the pyrazine ring. This is reflected in the two close NH···N contacts, 2.270 and 2.353 Å in **1a** and 2.354 Å in **2a**, which are significantly less than the sum of their van der Waals atomic radii (2.50 Å). Other conformers are found to lie slightly higher in energy than the global energy minimum (Figure 7). We note that our calculated structure of **2** (i.e., **2a**) is in excellent agreement with the observed X-ray structure, which adopts a conformation with the two pyrrole NH protons pointing away from each other.[42] Due to the close proximity of the two pyrrole rings, these receptor structures are significantly distorted from planarity. The calculated torsional angles of the pyrrole rings, with respect to the plane of the pyrazine ring, for all conformations are given in Figure 7. For **1a** and **2a**, the torsional angles are in the range 18−20°. Interestingly, a larger degree of nonplanarity is found for the less stable conformers (Figure 7). It is important to note that the pyrrolic NH protons bear strong charge, 0.47 and 0.45 for **1a**, and 0.46 for **2a**, respectively. Thus, both receptors **1** and **2** are characterized by two strong hydrogen-bond donor groups. We have also examined the rotational transition structure for interconversion of **2a** and **2b**. The computed barrier is just 24 kJ mol^{-1}, indicating that the pyrrole rings in **1** and **2** are relatively flexible in terms of rotation. It is important to note that these structures are strongly polar (calculated dipole moments are given in Figure 7). In particular, the "claw"-like systems (i.e., structures with two pyrrole NH protons facing each other), **1d** and **2c**, have a significantly higher dipole moment than the global energy minimum, **1a** and **2a**, respectively. Thus, one would expect these conformations to be differentially stabilized in the presence of a dielectric medium. In other words, the relative energies of **1d** and **2c** are expected to be smaller in the solution phase.

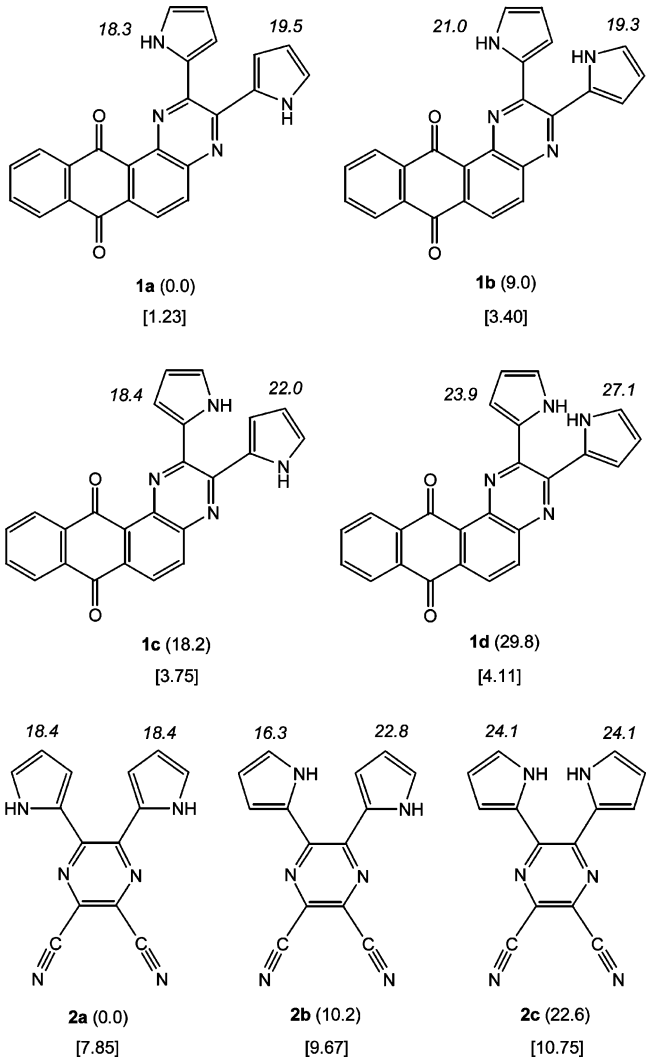

Figure 7. Structures of various conformations of receptors **1** (**1a**−**1d**) and **2** (**2a**−**2c**). Calculated B3LYP/6-311+G**//B3LYP/6-31G* + ZPE relative energies (kJ mol^{-1}) are given in parentheses; the torsional angles (in deg) of the pyrrole rings, with respect to the plane of pyrazine ring, are given in italics. Calculated (B3LYP/6-31G*) dipole moments (debye) are given in square brackets.

*3.3.2. Structures and Interaction Energies of **2**···X^- Complexes.* Next, we examine the structures and binding energies of the complexes between receptor **2** and halide ion X^- (X = F, Cl, and Br). Because there are two pyrrolic NH groups that could function as anion binding moieties, one may anticipate receptor **2** to interact with X^- to form stable 1:1 and 1:2 hydrogen-bonded **2**···X^- complexes, **6a** and **6b**, respectively (see Figure 8). In addition, both pyrrolic NH groups of **2** can orient in such a way that both NH protons can coordinate simultaneously with a halide ion to yield a "bidentate" complex

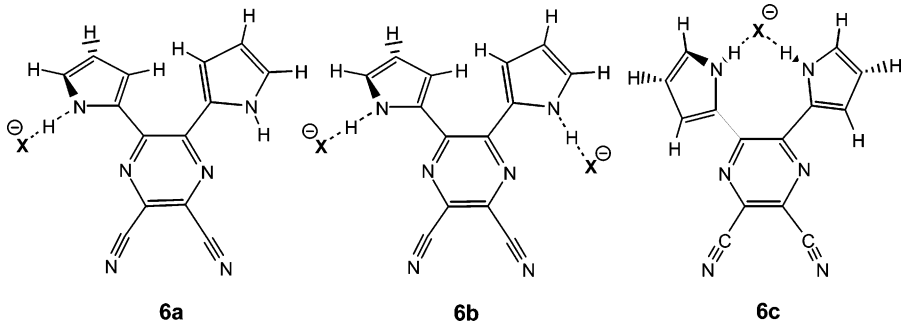

Figure 8. Structures of 1:1 (**6a** and **6c**) and 1:2 (**6b**) **2**···F^- complexes.

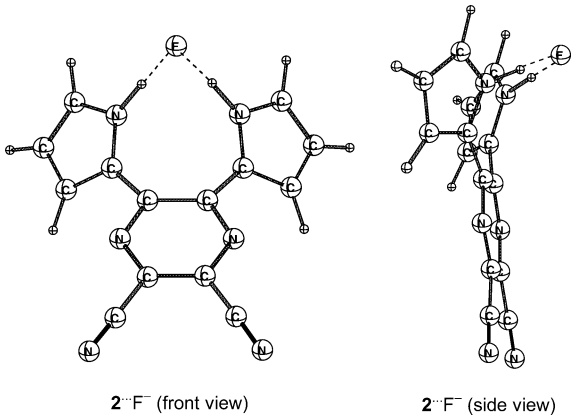

Figure 9. Optimized (B3LYP/6-31G*) structure of the **2**···F^- complex.

(**6c**, Figure 8). Of the two 1:1 complexes, the bidentate structure **6c** is significantly more stable than **6a** by 32 kJ mol^{-1}. This is not surprising as **6c** has two hydrogen-bond interactions while **6a** has only one. For the 1:2 complex (**6b**), the formation of a dianion is highly unfavorable because of the strong Columbic repulsion. Thus, the binding energy of the second fluoride ion, that is, **6a** → **6b**, is rather small, 10 kJ mol^{-1}. In summary, we predict that the preferred structure of the receptor−halide complex is in the form of a 1:1 bidentate complex **6c**, in accordance with the observed binding stiochiometry.

The optimized **2**···F^- bidentate structure is shown in Figure 9; the fluoride ion is bridged between the two pyrrole moieties via the NH···F hydrogen bonds. The interatomic distance between the fluoride anion and the pyrrole NH proton is 1.370 Å, while the N···HF angle is close to linearity (175.6°). The N−H bond lengths are lengthened significantly from 1.011 Å in **2** to 1.101 Å in the fluoride complex. These bonding parameters clearly show that the hydrogen bonds involved are particularly strong. Indeed, the computed interacting energy is substantial, 233 kJ mol^{-1} (ΔG_{298}) [Table 2]. In this intermolecular complex, both pyrrole subunits are strongly distorted from the plane of the pyrazine ring (torsional angle = 46.1°). Again, this indicates the pyrrole rings in **2** are sufficiently flexible with respect to rotation. The angle between the two sets of hydrogen bonds [α(H···F···H)] is 80°.

For the corresponding chloride and bromide complexes, the calculated binding affinities are considerably smaller, by 3−4 times (Table 2). The predicted order of halide affinity to **2** is F ≫ Cl > Br. This theoretical finding is in excellent accord with the experimental observation of the binding selectivity of F^- over Cl^-/Br^-. The major source of interaction energies of the receptor−halide complexes comes from the charged hydrogen bonding between the halide anion and the two pyrrolic NH protons. Hence, the trend of halide affinities toward **2** is readily understood in terms of the relative hydrogen-bond accepting ability of the halide ions. To provide further support to our argument, we investigated the hydrogen-bonded complexes (**4**···X^-) between pyrrole (**4**) and halide ions. As in the case of **2**, F^- shows a considerably stronger binding to pyrrole than Cl^- and Br^-. The trend of halide affinities in this series is the same as that calculated for **2** (Table 2). The binding energy of **2**···X^- is almost twice that in **4**···X^- (Table 2). In addition to the basicity of the halide ion, the geometrical complementarity between **2** and the halide ion may also play a significant role in governing the binding affinity. The fluoride anion is significantly smaller than the chloride and bromide ions and is, therefore, relatively easier to fit between the two pyrrole moieties of the receptor. This is readily reflected in the smaller NH···X and H···X···H angles and the larger degree of distortion of the pyrrole rings (ϕ) (see Table 3) in the chloride and bromide complexes.

TABLE 2: Calculated Interaction Energies[a] (ΔE_0, ΔH_{298}, and ΔG_{298}, in kJ mol^{-1}), Dipole Moments[b] (μ, debye), and NBO Atomic Charges of X (q_x)[c] of Various Receptor−Halide Ion Complexes

complex	X	ΔE_0	ΔH_{298}	ΔG_{298}[d]	μ	q_x
1···X^-	F	−222.1	−224.2	−191.2	9.87	−0.70
	Cl	−95.9	−96.4	−67.2	14.43	−0.81
	Br	−73.1	−72.9	−46.0	12.91	−0.81
2···X^-	F	−262.7	−264.9	−233.2	4.46	−0.69
	Cl	−131.4	−132.1	−103.5	6.46	−0.80
	Br	−109.3	−109.4	−82.4	5.38	−0.80
4···X^-	F	−165.1	−166.3	−138.6	2.70	−0.68
	Cl	−80.1	−81.1	−53.8	8.28	−0.89
	Br	−68.2	−68.8	−42.9	5.10	−0.89
5···X^-	F	−218.8	−220.9	−187.9	3.85	−0.70
	Cl	−100.4	−100.8	−72.2	7.86	−0.83
	Br	−79.5	−79.2	−52.9	6.19	−0.82

[a] Based on B3LYP/6-311+G**//B3-LYP/6-31G*+ZPE level. [b] B3LYP/6-31G* values. [c] Based on B3LYP/6-31G* wave function. [d] $\Delta G_{298} = \Delta H_{298} - 298^*\Delta S$.

Previous studies have shown that the hydrogen bond involving the anion is strong. For instance, FH···F^- complex has a large binding energy (ΔH_{298}) of 191.6 kJ mol^{-1}.[49] A detailed benchmark study by McAllister has shown that DFT calculations using hybrid functional, such as B3LYP, are in good accord with the ab initio methods (MP2, QCISD, and CCSD).[50] For the level of theory employed in this study (i.e., B3LYP/6-311+G**//B3LYP/6-31G*), the calculated binding energy in FH···F^- is 197.0 kJ mol^{-1} (ΔH_{298}), in very good agreement with the experimental estimate. This lends strong confidence to our predicted stabilization energies of the various receptor−anion complexes examined in this study.

To explore the effect of cyano substitution in **2**, we examined the halide complexes (**5**···X^-) of the parent analogue, that is, 2,3-di(1*H*-2pyrrolyl)-pyrazine (**5**). As expected, the calculated interaction energies are smaller than those of **2**···X^- (Table 2). Thus, our calculations confirm the enhanced halide anion binding affinity via attaching two cyano groups to the 5 and 6

TABLE 3: Calculated (B3LYP/6-31G*) Structural Parameters[a] of the Various Receptor−Halide Ion Complexes

complex	X	*d*(N−H)	*d*(NH···X)	α(NHX)	*τ*(NCCC)	α(H···X···H)
1···X^{-}[b]	F	1.099	1.375	173.6	−33.0	79.9
		1.100	1.375	176.3	49.3	
	Cl	1.038	2.099	167.6	−36.8	55.5
		1.039	2.089	173.4	52.4	
	Br	1.035	2.253	160.7	−36.1	51.4
		1.036	2.251	168.9	51.3	
2···X^{-}	F	1.101	1.370	175.6	42.6	80.2
	Cl	1.040	2.077	171.3	44.9	56.0
	Br	1.038	2.232	165.8	44.4	51.9
4···X^{-}	F	1.502	1.021	180.0		
	Cl	1.050	2.071	180.0		
	Br	1.046	2.246	180.0		
5···X^{-}	F	1.095	1.394	174.9	50.0	81.1
	Cl	1.037	2.120	172.6	53.5	57.4
	Br	1.035	2.277	168.7	54.0	54.0

[a] Bond lengths are in angstroms, and angles are in degrees. [b] Two sets of hydrogen bonds are different because of the asymmetry of the complex.

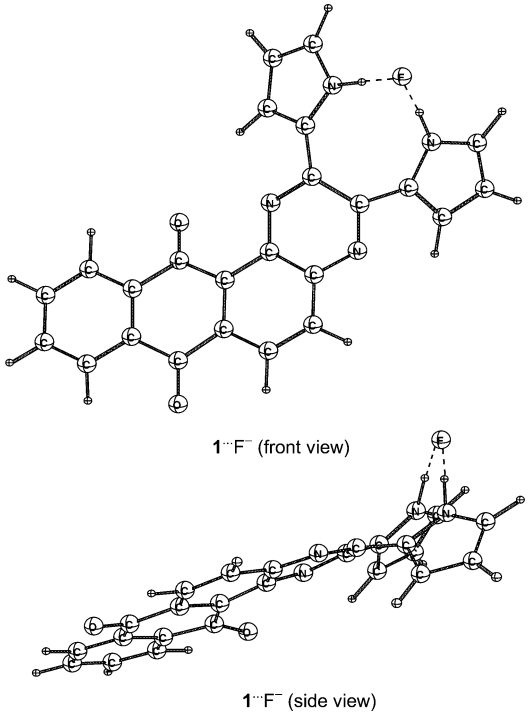

Figure 10. Optimized (B3LYP/6-31G*) structure of the **1**···F^{-} complex.

positions of the pyrazine ring in host **2**. The greater halide affinity in **2** relative to **5** can be rationalized in terms of the greater electron deficiency of the dicyano derivative, which leads to an increase in its hydrogen-bond-donating character. The use of the resonance-assisted approach, via conjugated multiple bond, is commonly employed to enhance the hydrogen-bond-donating ability of receptor. In accord with the smaller computed binding affinities, the geometrical parameters, NH···X distance and NH···X angle (Table 3), show weaker hydrogen bonds in **5**···X^{-}. Again, F^{-} binds with great affinity among the halides (Table 2).

3.3.3. Structures and Binding Energies of ***1***···*X*$^{-}$ *Complexes.* Finally, we consider the halide binding affinity of receptor **1**. As in the case of **2**···X^{-}, the "bidentate" type of structure is preferred in the **1**···X^{-} host−guest complex. The optimized geometry of the **1**···F^{-} complex is shown in Figure 10. It is characterized by the formation of two hydrogen bonds. However, these two sets of hydrogen-bonding interactions are slightly different in bond strengths because of the asymmetry of species **1**. The calculated structural parameters (Table 3) suggest that the hydrogen-bond strengths in **1**···X^{-} are less than those in **2**···X^{-}. In fact, the **1**···X^{-} complexes are predicted to have smaller binding energies (Table 2). For **1**···F^{-}, the computed interaction energy is 42 kJ mol^{-1} less than that of **2**···F^{-}. This theoretical finding is in excellent accord with the experimental observation that F^{-} has a larger binding constant with receptor **2** than **1**. The trend of the halide affinity of **1** is similar to those calculated for **2**, **4**, and **5**, that is, F ≫ Cl > Br.

Experimentally, the observed receptor−anion equilibria are reversed upon the addition of water. This is readily explained in terms of the fact that water competes for F^{-} at the pyrrolic NH hydrogen-bond-donating sites. For comparison, the calculated binding energy for a 1:1 water−fluoride ion complex (H_2O···F^{-}) is 117 kJ mol^{-1}.

It is worth noting that all of the receptor−halide ion complexes examined here are characterized by large dipole moments (Table 2), particularly for the chloride complexes. Thus, one would expect these complexes to be stabilized in a dielectric medium. These receptor−anion complexes may also be described as charge-transfer complexes. The calculated charge transfer (from anion to the receptor) for the complexes involving receptors **1** and **2** is rather uniform, ∼0.30 for the fluoride complexes and ∼0.20 for the chloride/bromide complexes (Table 2).

3.3.4. Calculated NMR and UV−Visible Spectra. The NMR spectra of receptors **1** and **2**, and their fluoride ion complexes, were computed using the GIAO method at the B3LYP/6-311+G(2d,p) level. First, we note that the calculated ^{1}H chemical shifts, with respect to TMS, of the NH protons of the two pyrrole moieties, 11.6 and 10.8 ppm in **1** and 9.3 ppm in **2**, are in pleasing agreement with the experimental values. In accordance with the experimental finding, a sizable shift to ∼20 ppm is predicted for both receptors, 20.6 and 20.3 ppm in **1** and 19.6 ppm in **2**, upon complexation with F^{-}. The large shifts that result from decreased shielding is readily attributed to the decreased electron density at the NH protons upon the formation of a hydrogen bond with F^{-}. Significant shifts are also predicted for the α and *β* protons on the pyrrole rings.

Both receptors **1** and **2** undergo a very dramatic color change in the presence of F^{-}. Furthermore, both systems display fluorescence emission spectra that are to all extents and purposes quenched in the presence of F^{-}. To understand the nature of the UV−visible spectral changes in the presence of halide ions, we calculated the absorption spectra of the receptors **2** and **5** and their complexes using the time-dependent DFT (TD-DFT) method at the B3LYP/cc-pVTZ level. The computed transition

TABLE 4: The Four Strongest UV Absorptions (T_1-T_4, >300 nm) for Receptors 2, 5, and Their Halide−Ion Complexes, Calculated at the TD-B3LYP/cc-pVTZ//B3LYP/6-31G* Level (Computed Transition Energies (TE) Are Given in nanometers)

	T_1		T_2		T_3		T_4	
species	TE	f[a]	TE	f[a]	TE	f[a]	TE	f[a]
2	429	0.105	421	0.239	344	0.119	321	0.434
2···F^-	469	0.138	467	0.030	403	0.134	378	0.460
2···Cl^-	456	0.021	455	0.102	399	0.115	374	0.456
2···Br^-	454	0.036	453	0.124	398	0.114	373	0.462
5	381	0.100	351	0.280	315	0.082		
5···F^-	389	0.084	367	0.018	339	0.218	307	0.190
5···Cl^-	377	0.083	362	0.019	332	0.176	306	0.160
5···Br^-	377	0.080	362	0.019	332	0.166	310	0.027

[a] Oscillator strength.

energies are summarized in Table 4. For sensor **2**, our computed transition energies of the two strongest peaks (321 and 421 nm) agree well with the observed values (338 and 427 nm, respectively). Upon complexation with F^-, both peaks undergo a significant blue shift, to 378 and 469 nm, respectively, in excellent accord with the observed spectral changes. Significantly smaller changes are predicted for the chloride and bromide complexes (Table 4). For the parent compound **5**, our calculations show that the UV absorption changes upon complexation with halide ion are significantly smaller. This again highlights the effectiveness of the cyano substitution in bringing the remarkable spectral changes. Hence, our computations confirm the experimental finding that **2** is an efficient colorimetric anion sensor.

4. Summary

In conclusion, dipyrrolyl derivatives **1** and **2** are easy-to-prepare, specific fluoride ion receptors, and they allow detection of F^- under visual as well as optical and electrochemical conditions in organic solvents. DFT calculations lend further support for the strong affinity and high selectivity of the fluoride ion for receptors **1** and **2**. Both receptors interact with a halide ion via hydrogen bonds with the pyrrolic NH protons in a bidentate fashion. The selectivity of F^- over Cl^- and Br^- is attributed to the fact that F^- is attributed to a better hydrogen-bond acceptor than Cl^- and Br^-. The computation of NMR and UV spectra confirms the experimental characterization of the receptor−anion complexes. Currently, we are engaged in the design and anion sensing studies of more such dipyrrolyl derivatives endowed with electron-withdrawing substituents.

Acknowledgment. B.G.M. and T.G. thank the Council of Scientific and Industrial Research, New Delhi, and Board of Research in Nuclear Sciences, Mumbai, for financial support of this work. The UPE Program of the University Grants Commission, New Delhi, is gratefully acknowledged for some of the instrumentation facilities. M.W.W. thanks the National University of Singapore for financial support. This collaboration was initiated at the Second Singapore-India Collaborative and Cooperative Symposium (SInCCCS-2) in Mumbai, 2003.

Supporting Information Available: Job plot analysis for the **2**···F^- complex (Figure S1) and ^1H NMR titration of **2** with TBAF in $CDCl_3$ (Figure S2). This material is available free of charge via the Internet at http://pubs.acs.org.

References and Notes

(1) Stryer, L. *Biochemistry*, 4th ed.; W. H. Freeman & Co.: New York, 1995.

(2) *Riegel's Handbook of Industrial Chemistry*, 9th ed.; Kent, J. A., Ed.; Van Nostrad Reinhold-International Thomson Publishing: New York, 1992.

(3) *Ullmann's Encyclopedia of Industrial Chemistry*, 6th ed.; Bailey, J. E., Bohnet, M., Brinker, C. J., Cornils, B., Evans, T., Greim, H., Hegedus, L. L., Heitbaum, J., Keim, W., Kleemann, A., Kreysa, G., Loliger, J., McGuire, J. L., Mitsutani, A., Plass, L., Stephanopoulos, G., Werner, D., Woditsch, P., Yoda, N., Eds.; 1999 Electronic Release; Wiley VCH: New York, 1999.

(4) Atwood, J. L.; Steed, J. W. *Supramol. Chem. Anions* **1997**, 147.

(5) Beer, P. D.; Gale, P. A. *Angew. Chem., Int. Ed.* **2001**, *40*, 486.

(6) Kirk, K. L. *Biochemistry of the Halogens and Inorganic Halides*; Plenum Press: New York, 1991; p 58.

(7) Kleerekoper, M. *Endochrinol. Metab. Clin. North Am.* **1998**, *27*, 441.

(8) Wiseman, A. *Handbook of Experimental Pharmacology* XX/2, Part 2; Springer-Verlag: Berlin, 1970; pp 48−97.

(9) Nielsen, K. A.; Jeppesen, J. O.; Levillain, E.; Becher, J. *Angew. Chem., Int. Ed.* **2003**, *42*, 187.

(10) Miyaji, H.; Sato, W.; Sessler, J. L. *Angew. Chem., Int. Ed.* **2000**, *39*, 1777.

(11) Black, C. B.; Andrioletti, B.; Try, A. C.; Ruiperez, C.; Sessler, J. L. *J. Am. Chem. Soc.* **1999**, *121*, 10438.

(12) Anzenbacher, P., Jr.; Try, A. C.; Miyaji, H.; Jursikova, K.; Lynch, V. M.; Marquez, M.; Sessler, J. L. *J. Am. Chem. Soc.* **2000**, *122*, 10268.

(13) Mizuno, T.; Wei, W.-H.; Eller, L. R.; Sessler, J. L. *J. Am. Chem. Soc.* **2002**, *124*, 1134.

(14) Anzenbacher, P., Jr.; Tyson, D. S.; Jursikova, K.; Castellano, F. N. *J. Am. Chem. Soc.* **2002**, *124*, 6232.

(15) Sessler, J. L.; Maeda, H.; Mizuno, T.; Lynch, V. M.; Furuta, H. *Chem. Commun.* **2002**, 862.

(16) Sessler, J. L.; Maeda, H.; Mizuno, T.; Lynch, V. M.; Furuta, H. *J. Am. Chem. Soc.* **2002**, *124*, 13474.

(17) Aldakov, D.; Anzenbacher, P., Jr. *Chem. Commun.* **2003**, 1394.

(18) Ghosh, T.; Maiya, B. G. *Proc. Indian Acad. Sci.* (*Chem. Sci.*) **2004**, *116*, 17.

(19) To the best of our knowledge, structures of any DPQ-based receptors and their anion complexes have not been investigated by quantum mechanical calculations so far.

(20) Perrin, D. D.; Armarego, W. L. F.; Perrin, D. R. *Purification of Laboratory Chemicals*; Pergamon Press: New York, 1980.

(21) Behr, D.; Brandange, S.; Lindstrom, B. *Acta Chem. Scand.* **1973**, *27*, 2411.

(22) Quimby, D. J.; Lango, F. R. *J. Am. Chem. Soc.* **1975**, *97*, 5111.

(23) Berlman, I. B. *Handbook of Fluorescence Spectra of Aromatic Molecules*, 2nd ed.; Academic Press: New York, 1971; p 322.

(24) Reddy, D. R.; Maiya, B. G. *J. Phys. Chem. A* **2003**, *107*, 6326.

(25) Sastri, C. V.; Eswaromoorthy, D.; Giribabu, L.; Maiya, B. G. *J. Inorg. Biochem.* **2003**, *94*, 138.

(26) Hariprasad, G.; Dahal, S.; Maiya, B. G. *J. Chem. Soc., Dalton Trans.* **1996**, 3429.

(27) Ambroise, A.; Maiya, B. G. *Inorg. Chem.* **2000**, *39*, 4256.

(28) Ambroise, A.; Maiya, B. G. *Inorg. Chem.* **2000**, *39*, 4264.

(29) Connors, A. K. *Binding Constants: The Measurement of Molecular Complex Stability*; Wiley−VCH: New York, 1987.

(30) Becke, D. A. *J. Chem. Phys.* **1993**, *98*, 5648.

(31) Lee, C.; Yang, W.; Parr, R. G. *Phys. Rev. B* **1988**, *37*, 785.

(32) Wong, M. W. *Chem. Phys. Lett.* **1996**, *256*, 391.

(33) *NIST-JANAF Thermochemical Tables*, 4th ed.; Chase, M. W., Ed.; National Institute of Standards and Technology: New York, 1998.

(34) Boys, S. F.; Bernardi, F. *Mol. Phys.* **1970**, *19*, 553.

(35) Reed, A. E.; Curtiss, L. A.; Weinhold, F. *Chem. Rev.* **1988**, *88*, 899.

(36) Messerschmidt, M.; Wagner, A.; Wong, M. W.; Luger, P. *J. Am. Chem. Soc.* **2002**, *124*, 732.

(37) Wolinski, K.; Hinton, J. F.; Pulay, P. *J. Am. Chem. Soc.* **1990**, *112*, 8351.

(38) Cheeseman, J. R.; Trucks, G. W.; Keith, T.; Frisch, M. J. *J. Phys. Chem.* **1996**, *104*, 5497.

(39) Bauernschmitt, R.; Ahlrichs, R. *Chem. Phys. Lett.* **1996**, *256*, 454.

(40) Casida, M. E.; Jamorski, C.; Casida, K. C.; Salahub, D. R. *J. Chem. Phys.* **1998**, *108*, 4439.

(41) Frisch, M. J.; Trucks, G. W.; Schlegel, H. B.; Scuseria, G. E.; Robb, M. A.; Cheeseman, J. R.; Zakrzewski, V. G.; Montgomery, J. A., Jr.; Stratmann, R. E.; Burant, J. C.; Dapprich, S.; Millam, J. M.; Daniels, A. D.; Kudin, K. N.; Strain, M. C.; Farkas, O.; Tomasi, J.; Barone, V.; Cossi, M.; Cammi, R.; Mennucci, B.; Pomelli, C.; Adamo, C.; Clifford, S.; Ochterski, J.; Petersson, G. A.; Ayala, P. Y.; Cui, Q.; Morokuma, K.; Malick, D. K.; Rabuck, A. D.; Raghavachari, K.; Foresman, J. B.; Cioslowski, J.; Ortiz, J. V.; Stefanov, B. B.; Liu, G.; Liashenko, A.; Piskorz, P.; Komaromi, I.; Gomperts, R.; Martin, R. L.; Fox, D. J.; Keith, T.; Al-Laham, M. A.; Peng, C. Y.; Nanayakkara, A.; Gonzalez, C.; Challacombe, M.; Gill, P. M. W.; Johnson, B.; Chen, W.; Wong, M. W.; Andres, J. L.; Gonzalez, C.;

Head-Gordon, M.; Replogle, E. S.; Pople, J. A. *Gaussian 98*; Gaussian, Inc.: Pittsburgh, PA, 1998.

(42) While this manuscript was being prepared, the synthesis and characterization of receptor **2** and a few of its derivatives have been reported by Sessler et al. (Sessler, J. L.; Pantos, G. D.; Katayev, E.; Lynch, V. M. *Org. Lett.* **2003**, *5*, 4141). However, the fluoride ion sensing ability of **2** or of its derivatives was not presented in that paper.

(43) Dickenson, J. E.; Summers, L. A. *Aust. J. Chem.* **1970**, *23*, 1023.

(44) Amouyal, E.; Homsi, A.; Chambron, J. C.; Sauvage, J. P. *J. Chem. Soc., Dalton Trans.* **1990**, 1841.

(45) Nicholson, R. S.; Shain, I. *Anal. Chem.* **1964**, *36*, 706.

(46) The addition of a large excess of $TBAPF_6$ to DMF solutions containing **1** or **2** did not result in changes in their color and spectral (UV−visible and fluorescence) properties, indicating that this anion does not bind to these receptors.

(47) Medina, J. C.; Goodnow, T. T.; Rojas, M. T.; Atwood, J. L.; Lynn, B. C.; Kaifer, A. E.; Gokel, G. W. *J. Am. Chem. Soc.* **1992**, *114*, 10583.

(48) Beer, P. D.; Gale, P. A.; Chen, G. Z. *J. Chem. Soc., Dalton Trans.* **1999**, 1897.

(49) Wenthold, P. G.; Squires, R. R. *J. Phys. Chem.* **1985**, *99*, 2002.

(50) McAllister, M. A. *J. Mol. Struct. (THEOCHEM)* **1998**, *427*, 39.